11-1997

Phase Jitter in MPSK Carrier Tracking Loops: Analytical, Simulation and Laboratory Results

Brian T. Kopp

William P. Osborne
osborne@engr.siu.edu

Phase Jitter in MPSK Carrier Tracking Loops: Analytical, Simulation, and Laboratory Results

Brian T. Kopp, *Member, IEEE*, and William P. Osborne, *Senior Member, IEEE*

***Abstract*— A performance characteristic of *M*-ary phase shift keying (MPSK) receivers is the variance of the phase error between the received and recovered signal carriers. For binary phase shift keying (BPSK) and quadrature phase shift keying (QPSK) loops utilizing integrate and dump filters and operating in the linear region, closed-form solutions for this variance exist [1], [2]. In this paper the variance is found by numerical methods for $M > 4$. For verification and to investigate operation in the nonlinear region, computer simulation and hardware modeling were used [3].**

***Index Terms*—BPSK, carrier tracking loops, equivalent noise, loop bandwidth, MPSK, phase detector, phase detector gain, phase jitter, phaselock loops, PSK, QPSK, self noise, squaring loss, variance of phase error.**

I. Introduction

PHASE JITTER is the most important design parameter in a carrier tracking loop. Analytical results are available for predicting phase jitter in binary phase shift keying (BPSK) and quadrature phase shift keying (QPSK) loops, but there are no results available for *M*-ary phase shift keying (MPSK). This paper addresses the jitter in MPSK carrier loops for $M > 4$. To study this phenomenon the quadrature crossover feedback receiver configured for MPSK operation and utilizing integrate and dump arm filters is considered. The baseband model of this loop is shown in Fig. 1, from which a transfer function relating the phase error to the equivalent noise in the loop can be derived. The noise components in the equivalent noise N_I and N_Q are the noise samples from the quadrature correlators. Each are Gaussian with variance $N_0/2E$ where E is the MPSK symbol energy and the two-sided power spectral density of the channel noise is $N_0/2$. Note that perfect automatic gain control has been assumed, i.e., the signal magnitude is assumed to be unity. The desired transfer function for the second order loop is [1]

$$H_n(s) = \frac{K_o(s+a)}{s^2 + \alpha_{\rm SNR} K_o(s+a)} = \frac{1}{\alpha_{\rm SNR}} H(s) \quad (1)$$

and $\alpha_{\rm SNR}$ is the signal-to-noise ratio (SNR)-dependent phase detector gain. This term reflects the fact that at low SNR's, when bad data decisions are being made, the phase detector, in effect, has less signal to track on. Therefore $0 < \alpha_{\rm SNR} \le 1$ with the upper limit corresponding to high-SNR operation.

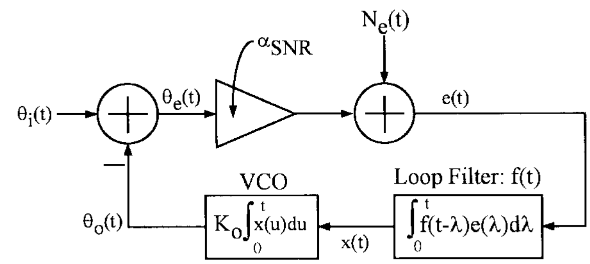

Fig. 1. The linear baseband model.

The variance of the phase error is obtained by relating the input and the output power spectral densities through the linear system of (1) and is given by [1]

$$\sigma^2_{\theta_e} = \frac{B_L}{S\_R} \frac{\sigma^2_{N_e}}{\alpha^2_{\rm SNR}} \quad (2)$$

where B_L/S_R is the ratio of the loop bandwidth to the MPSK symbol rate and $\sigma^2_{N_e}$ is the variance of the equivalent noise in the loop.[1] All three components are a function of SNR.

For MPSK in general, a closed-form solution to the variance of the equivalent noise is unavailable. However, a numerical solution can be obtained for any M by the following process: Express the variance of the equivalent noise, in terms of the two-dimensional noise components N_I and N_Q and the transmitted modulation angle θ_m as

$$\sigma^2_{N_e} = E\big[N_e(t)^2\big] = \int_{-\infty}^{\infty}\int_{-\infty}^{\infty}\int_{-\infty}^{\infty} g(N_I, N_Q, \theta_m) f(N_I)f(N_Q)h(\theta_m)dN_I dN_Q d\theta_m \quad (3)$$

where

$$g(N_I, N_Q, \theta_m) = [N_I\hat{Q} - N_Q\hat{I}]^2 \quad (4)$$

$f(\bullet)$ is the Gaussian probability density function (pdf) and $h(\bullet)$ is the transmitted modulation angle pdf. If equally likely transmitted symbols are assumed, (3) reduces to

$$\sigma^2_{N_e} = \int_{-\infty}^{\infty}\int_{-\infty}^{\infty} g(N_I, N_Q, \theta_m = 0) f(N_I)f(N_Q)dN_I dN_Q \quad (5)$$

where the zero modulation angle has been assumed. The variance of the equivalent noise is obtained by the numerical integration of (5). It is then possible to express the variance

[1] The equivalent noise is cyclostationary. See Hinedi and Lindsey [1] for further discussion.

Paper approved by P. H. Wittke, the Editor for Communication Theory of the IEEE Communications Society. Manuscript received January 26, 1995; revised September 30, 1996 and April 4, 1997.

B. T. Kopp was with New Mexico State University, Las Cruces, NM 88003 USA. He is now with the Semaphore Group, Fernandina Beach, FL 32035 USA (e-mail: bkopp@gate.net).

W. P. Osborne was with New Mexico State University, Las Cruces, NM 88003 USA. He is now with the College of Engineering, University of Texas-Dallas, Richardson, TX 75083-0688 USA.

Publisher Item Identifier S 0090-6778(97)08200-7.

in terms of the self-noise ξ (a function of SNR) and the SNR itself, as

$$\sigma_{N_e}^2 = \frac{N_o}{2E}\xi. \tag{6}$$

Note that self-noise in a decision-directed loop refers to the effect at low SNR's of making bad decisions on the noise inside the loop. At high SNR's the self-noise for any M is unity. Further, BPSK exhibits unity self-noise for any SNR, and for QPSK a closed-form [1] solution exists. To find the self-noise for $M > 4$, and at any SNR, divide the result of the numerical integration of (5) by the high SNR approximation to (6).

The next component of interest in the calculation of the variance of the phase error is the phase detector gain, which is the partial derivative, with respect to phase error, of the phase detector characteristic evaluated at zero phase error. This characteristic can be expressed in terms of the transmitted modulation angle, data estimates, and phase error as [4]

$$\mathrm{PD}(\theta_e) = E[\cos(\theta_e - \theta_m)\hat{Q} + \sin(\theta_e - \theta_m)\hat{I}. \tag{7}$$

Noting that $\hat{Q}$, $\hat{I}$, and θ_m are discreet random variables, and assuming that the data symbols are equally likely, (7) becomes

$$\mathrm{PD}(\theta_e) = \sum_{j=0}^{M-1} \sin(\theta_e + \hat{\theta}_{mj}) P(\hat{\theta}_{mj} \mid \theta_m = 0, \theta_e). \tag{8}$$

The conditional probability in (8) is computed by integrating the conditional density that describes the probability of receiving a particular phase γ given $\theta_m = 0$ over the decision region of phase that corresponds to the received modulation angle. The density is configured to account for a phase error θ_e and is expressed as [5]

$$\begin{aligned} p(\gamma \mid \theta_m = 0, \theta_e) &= \frac{e^{-\frac{E}{N_o}}}{2\pi}\left[1 + \sqrt{\frac{4E\pi}{N_o}}\cos(\gamma+\theta_e)e^{-\frac{E}{N_o}\cos^2(\gamma+\theta_e)}\right. \\ &\quad \left. \times\, Q\left(-\sqrt{\frac{2E}{N_o}}\cos(\gamma+\theta_e)\right)\right]. \end{aligned} \tag{9}$$

Using (8) and (9), the phase detector characteristic is calculated numerically.

Assuming a damping factor ζ and natural frequency ω_n, the loop noise bandwidth of the loop in Fig. 1 is given by

$$B_{L_{\text{CLASSICAL}}} = \omega_n\left(\zeta + \frac{1}{4\zeta}\right) \tag{10}$$

which can be rewritten as

$$B_L = \mu_{\text{SNR}} B_{L_{\text{HIGHSNR}}} = \mu_{\text{SNR}}\omega_n\left(\zeta + \frac{1}{4\zeta}\right) \tag{11}$$

where

$$\mu_{\text{SNR}} = \frac{(\alpha_{\text{SNR}}4\zeta^2 + 1)}{(4\zeta^2 + 1)} \tag{12}$$

is the loop bandwidth compression factor. Using (2), (6), and (11), the variance of phase error is expressed as

$$\sigma_{\theta_e}^2 = \frac{N_o}{2E}\frac{B_{L_{\text{HIGHSNR}}}}{S\_R}\mu_{\text{SNR}}\frac{\xi}{\alpha_{\text{SNR}}^2}. \tag{13}$$

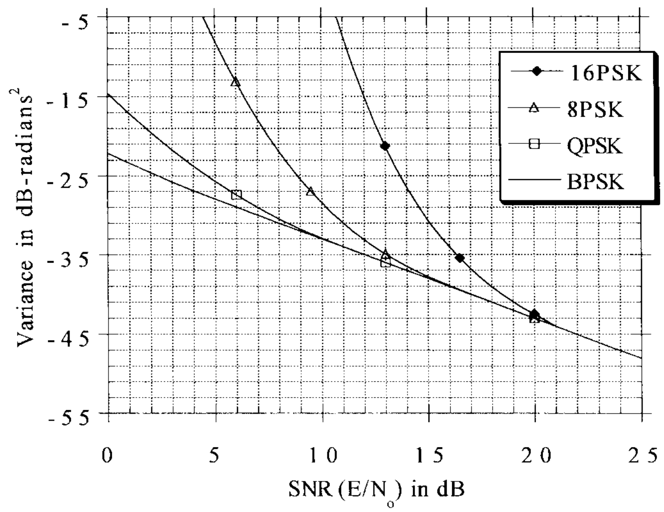

Fig. 2. Calculated variance of phase error.

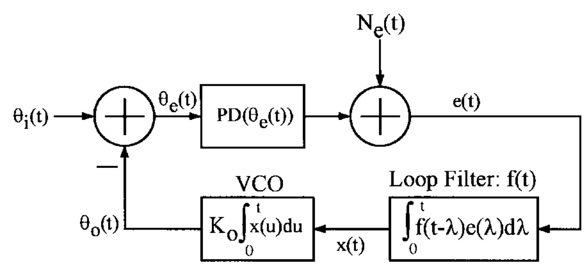

Fig. 3. The nonlinear baseband model.

The variance of phase error data is shown for BPSK through 16 PSK in Fig. 2. The variance is displayed for a high-SNR loop bandwidth-to-symbol rate ratio of 1.0%. Unity loop damping was selected for these analytical results.

II. Simulation and Hardware Results

To verify the numerical results, computer simulations were conducted using the nonlinear baseband model of Fig. 3. As a second means of verifying the variance of the phase error, an MPSK carrier tracking loop was constructed in hardware. Fig. 4 provides a block diagram of the hardware testset. A simulated MPSK transmission was created and used as an input to the loop. In fact, just as was done with the numerical analysis and the computer simulations, the MPSK transmission represented the transmission of the same symbol continuously. This made the MPSK signal a continuous-wave (CW) carrier signal that could be obtained from a standard frequency synthesizer and it removed the impact of intersymbol interference as a dependent variable in the testing. White noise was added to the CW carrier signal and the result passed to the demodulator front end of the carrier tracking loop. This demodulator front end is a quadrature structure that power-divides the CW carrier-with-noise signal into two signals that are mixed in quadrature with the voltage-controlled oscillator (VCO) signal. The outputs of the quadrature mixers are fed through a set of low-pass filters. Analog-to-digital conversion takes place after the low-pass filters and the generated 8 bits of I channel baseband data

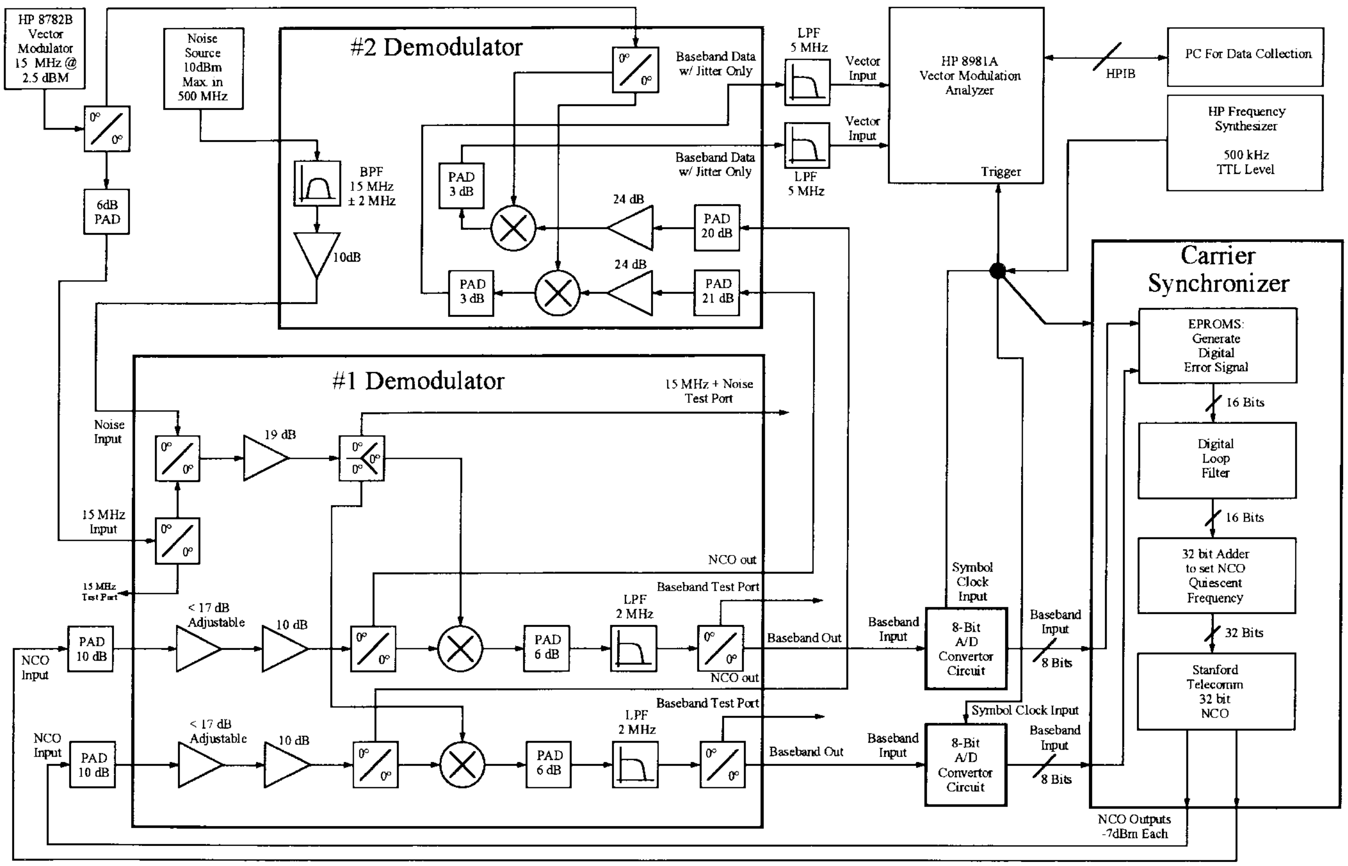

Fig. 4. The MPSK high-SNR carrier tracking hardware test configuration.

and 8 bits of Q channel baseband data are passed to a lookup table which generates the error signal of the loop. This error signal is processed by a digital filter that creates a second-order transfer function for the loop. The output from the digital filter is added to the carrier frequency of the output sinusoid from the loop's numerically controlled oscillator (NCO). The NCO creates two analog quadrature sinusoids which return to the demodulator front end.

The I and Q baseband data at the output of the low-pass filters are corrupted by the input channel noise and, thus, variance measurements cannot be made using these data. To facilitate making variance measurements, the outputs from the NCO are mixed in quadrature with the "clean" CW carrier from the synthesizer. The low-pass-filtered mixer outputs are corrupted only with phase jitter from the NCO. Large sample sets of this I and Q data were taken using a modulation analyzer; thus, any correlation between adjacent samples was averaged out. Fig. 5 shows plots of the 8 PSK through 16 PSK theory, simulation, and hardware results, respectively. QPSK theory and simulation data are provided for reference. Tests were conducted for $M = 2$ through $M = 16$ and over various high-SNR loop bandwidth-to-symbol rate ratios.

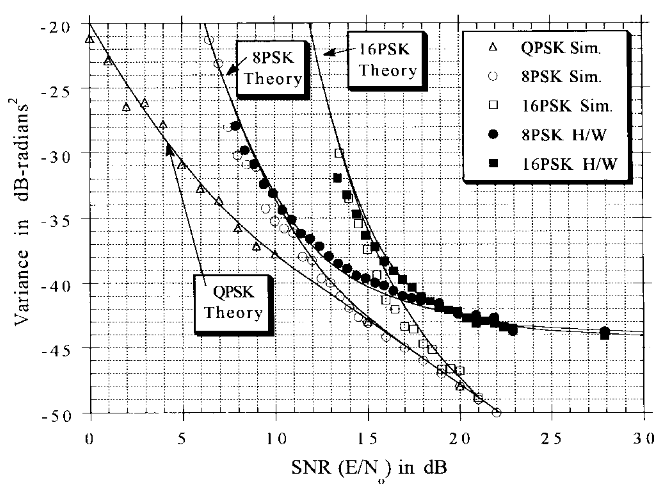

Fig. 5. Variance of phase error simulation and hardware data.

III. Discussion of Results

As the simulation and hardware data indicate, there is substantial verification of the general solution used to calculate the variance of the phase error. With the exception of a few samples, all of the simulation data falls within a 95% confidence interval. Before the validity of the hardware results can be discussed, an interesting phenomenon in that data must be addressed. This phenomenon is the horizontal flare in the hardware variance curves, indicating the presence of a phase jitter floor. This floor is a result of phase jitter in the NCO, which is unaccounted for in the analysis. This phase noise floor in the hardware dominates the results at high SNR's only. At low SNR's the variance in the phase error data is accurately reflecting the mechanism of interest, i.e., the overall loss in performance due to making incorrect data decisions in the carrier tracking loop. When the MPSK general solution data are "corrected" by adding to them the phase noise floor present in the hardware, the results are accurate at all SNR's. These curves are also shown in Fig. 5 and follow the hardware results.

In the plots of simulation data and hardware data for 8 PSK and 16 PSK, the lowest SNR at which a data point is plotted represents the minimum SNR for which phaselock can be maintained. A striking result in this data is that the point at which phaselock terminates seems to be a weak function of loop bandwidth and a strong function of E/N_o. For both 8 PSK and 16 PSK, the simulation and hardware data that was collected cover a 5.4-dB range of high-SNR loop bandwidth-to-symbol rate ratios (from 0.19% to 0.66%). However, the phaselock threshold moves at most 1.6 dB for the 8 PSK hardware results and not at all for the 16 PSK simulation results.

REFERENCES

[1] S. Hinedi and W. Lindsey, "On the self-noise in QASK decision-feedback carrier tracking loops," *IEEE Trans. Commun.*, vol. 37, pp. 387–392, Apr. 1989.

[2] J. H. Yuen, *Deep Space Telecommunications Systems Engineering*. New York: Plenum, 1983, pp. 179–333.

[3] B. Kopp, "An analysis of carrier phase jitter in an MPSK receiver utilizing MAP estimation," Ph.D. dissertation, New Mexico State University, Las Cruces, NM, pp. 163–191, May 1994.

[4] W. Osborne and B. Kopp, "Synchronization in M-PSK modems," in *SUPERCOMM/ICC*, 1992, pp. 348.6.1–348.6.5.

[5] R. D. Parsons and S. G. Wilson, "Polar quantizing for coded PSK transmission," *IEEE Trans. Commun.*, vol. 38, pp. 1511–1519, Sept. 1990.